Electronic Supplementary Information (ESI)

Non-stackable molecules assemble into porous crystals displaying concerted cavity-changing motions

Taewon Kang,[†,∥] Hongsik Kim,[†,∥] Sungeun Jeoung,[‡,∥] Dohyun Moon,[§,*] Hoi Ri Moon,[‡,*] and Dongwhan Lee[†,*]

[†]*Department of Chemistry, Seoul National University, 1 Gwanak-ro, Gwanak-gu, Seoul 08826, Korea*
[‡]*Department of Chemistry, Ulsan National Institute of Science and Technology (UNIST), 50 UNIST-gil, Eonyang-eup, Ulji-gun, Ulsan 44919, Korea*
[§]*Beamline Division, Pohang Accelerator Laboratory, 80 Jigokro-127-beongil, Nam-gu, Pohang 37673, Korea*
[∥]These authors contributed equally
*e-mail: dmoon@postech.ac.kr; hoirimoon@unist.ac.kr; dongwhan@snu.ac.kr

Table of Contents

Experimental Section

1) General Information

General Considerations. Unless otherwise noted, all reagents were purchased from commercial suppliers and used as received. Toluene used for synthesis of the compound **1** was saturated with nitrogen and purified by passage through activated Al_2O_3 columns under nitrogen (Innovative Technology SPS PureSolv MD4). The compound **TI** was synthesized according to the previously reported procedure.[1] All air-sensitive manipulations were carried out under argon atmosphere by standard Schlenk-line techniques.

Physical Measurements. ^{1}H NMR and ^{13}C NMR spectra were recorded on a 850 MHz Bruker AnNACE III HD spectrometer or a 300 MHz Bruker Advance DPX-300 spectrometer. Chemical shifts were referenced to the residual solvent peaks.[2] High-resolution electrospray ionization (ESI) mass spectra were obtained on an ESI-Q-TOF mass spectrometer (Compact, Bruker Daltonics Inc) at the Organic Chemistry Research Center at Sogang University. FT-IR spectra were recorded on a PerkinElmer Spectrum Two N FT-NIR Spectrometer. Gas adsorption and desorption isotherms were recorded on a BELSORP-max. Powder XRD patterns were recorded on a Rayonix MX225HS CCD area detector diffractometer using synchrotron radiation (BL2D-SMC at PLSII, $\lambda = 1.20000$ Å) or LYNXEYE XE detector using CuKα radiation ($\lambda = 1.5406$ Å). Melting points were measured by IA9100 melting point apparatus (Barnstead International).

Gas Sorption Studies. The gas adsorption–desorption isotherms were obtained using a BELSORP-max. Prior to adsorption measurements, bulk powder samples of **1** (ca 50 mg) was evacuated ($P < 10^{-5}$ mbar) at r.t. for 24 h or at 100 °C for 3 h. The pore size distribution curve, derived from the adsorption branch of nitrogen isotherm at 77 K, was analyzed by using nonlocal density functional theory (NLDFT).[3]

---

[1] T. Kang, H. Kim and D. Lee, Triazoliptycenes: A twist on iptycene chemistry for regioselective cross-coupling to build nonstacking fluorophores. *Org. Lett.*, 2017, **19**, 6380–6383.

[2] G. R. Fulmer, A. J. M. Miller, N. H. Sherden, H. E. Gottlieb, A. Nudelman, B. M. Stoltz, J. E. Bercaw and K. I. Goldberg, NMR chemical shifts of trace impurities: Common laboratory solvents, organics, and gases in deuterated solvents relevant to the organometallic chemist. *Organometallics*, 2010, **29**, 2176–2179.

[3] G. Kupgan, T. P. Liyana-Arachchi and C. M. Colina, NLDFT pore size distribution in amorphous microporous materials. *Langmuir*, 2017, **33**, 11138–11145.

2) Computations and Simulations

Molecular Electrostatic Potential (MEP) Map of 1. Geometry optimization of the molecule was performed with Gaussian '09 Revision E.01 software.[4] The MEP map was generated on the geometry-optimized structure of **1** (B3LYP/6-31G(d) level).

Simulation of Powder X-Ray Diffraction (PXRD) Pattern. Simulated PXRD patterns were generated with the Mercury software using CIF files obtained without squeezing the solvent molecules ($\lambda = 1.20000$ Å).

Hirshfeld Surface of 1. Hirshfeld surfaces of solvent-squeezed **1A** and **1B** mapped with d_{norm} and corresponding fingerprint plots were calculated by using Crystal Explorer 17.5.[5]

---

[4]M. J. Frisch, G. W. Trucks, H. B. Schlegel, G. E. Scuseria, M. A. Robb, J. R. Cheeseman, G. Scalmani, V. Boarone, B. Mennucci, G. A. Petersson, *et al.* Gaussian '09 , revision E.01; Gaussian, Inc.: Wallingford CT, 2009.

[5]M. A. Spackman and D. Jayatilaka, Hirshfeld surface analysis. *CrystEngComm*, 2009, **11**, 19–32.

3) Synthetic Procedures

Compound 1. A 4-mL shell vial was charged with $Pd_2(dba)_3$ (5.7 mg, 0.0062 mmol) and $Me_4tBuXPhos$ (7.4 mg, 0.015 mmol) in the glovebox with argon atmosphere. Dry toluene (0.4 mL) was delivered via syringe. The resulting mixture was heated at 120 °C for 5 min. A separate 4-mL vial was loaded with **TI** (200 mg, 0.815 mmol), 1,4-dibromobenzene (81 mg, 0.34 mmol), and K_3PO_4 (174 mg, 0.817 mmol). The reaction vessel was sealed with a screw septum, and evacuated and backfilled with argon three times. Dry toluene (1.2 mL) and the pre-mixed catalyst solution was delivered via syringe. The reaction mixture was heated at 120 °C for 17 h under argon atmosphere. The reaction mixture was cooled to r.t., and purified by flash column chromatography on SiO_2 (eluent: CH_2Cl_2). The isolated solid material was washed with EtOAc/hexane mixed-solvent (1:1, v/v, 25 mL) to afford **1** as a white solid (161 mg, 0.286 mmol, yield = 83%). ^{1}H NMR (500 MHz, CDCl$_3$, 298 K): δ 7.90 (s, 2H), 7.42 (dd, J = 5.4, 3.2 Hz, 4H), 7.04 (dd, J = 5.4, 3.2 Hz, 4H), 5.57 (s, 2H). ^{13}C NMR (125 MHz, CDCl$_3$, 298 K): δ 157.31, 144.62, 138.48, 126.10, 124.61, 118.90, 46.84. FT-IR (ATR, cm^{-1}): 3069, 3001, 2923, 2853, 1919, 1680, 1524, 1487, 1456, 1433, 1418, 1340, 1316, 1243, 1192, 1177, 1158, 1148, 1100, 1022, 981, 943, 911, 894, 869, 835, 788, 749, 741, 639, 622. HRMS (ESI, m/z) calcd. for $C_{38}H_{25}N_6$ [M + H]$^+$ 565.2135, found 565.2137. m.p. > 400 °C.

Compound 2. A 4-mL shell vial was charged with $Pd_2(dba)_3$ (7.8 mg, 0.0085 mmol) and $Me_4tBuXPhos$ (10.1 mg, 0.021 mmol) in the glovebox with argon atmosphere. Dry toluene (0.2 mL) was delivered via syringe. The resulting mixture was heated at 120 °C for 5 min. A separate 4-mL vial was loaded with **TI** (296 mg, 1.21 mmol), 1,3-dibromobenzene (121 mg, 0.51 mmol), and K_3PO_4 (281 mg, 2.06 mmol). The reaction vessel was sealed with a screw septum, and evacuated and backfilled with nitrogen three times. Dry toluene (2.5 mL) and the pre-mixed catalyst solution was delivered via syringe. The reaction mixture was heated at 120 °C for 23 h under argon atmosphere. The reaction mixture was cooled to r.t., diluted with CH_2Cl_2 (150 mL), and washed with brine (50 mL). The organic fraction was dried over $MgSO_4$, filtered, and evaporated under reduced pressure. The resulting crude mixture was purified by flash column chromatography on SiO_2 (eluent: CH_2Cl_2/hexane (1:1, v/v) → CH_2Cl_2 only) to afford **2** as a white solid (201 mg, 0.356 mmol, yield = 70%). ^{1}H NMR (850 MHz, CDCl$_3$, 298 K): δ 8.48 (t, J = 2.0 Hz, 1H), 7.70 (dd, J = 8.2, 2.0 Hz, 2H), 7.43 (m, 8H), 7.36 (t, J = 8.2 Hz, 1H), 7.05 (m, 8H), 5.57 (s, 4H). ^{13}C NMR (214 MHz, CDCl$_3$, 298 K): δ 157.13, 144.46, 141.13, 129.96, 125.98, 124.49, 115.11, 108.08, 46.70. FT-IR (ATR, cm^{-1}): 3007, 2923, 2052, 1734, 1648, 1607, 1554, 1505, 1484, 1472, 1456, 1417, 1361, 1328, 1316, 1271, 1244, 1219, 1190, 1180, 1158, 1090, 1062, 1021, 948, 912, 877, 850, 828, 771, 748, 725, 680, 649, 634, 620. HRMS (ESI, m/z) calcd. for $C_{38}H_{24}N_6Na$ [M + Na]$^+$ 587.1955 , found 587.1958. This compound thermally degrades at around T = 375–380 °C to a dark brown material, which melts at T $\approx$ 390 °C.

Compound 3. A 4-mL shell vial was charged with $Pd_2(dba)_3$ (4.1 mg, 0.0045 mmol) and $Me_4tBuXPhos$ (5.2 mg, 0.011 mmol) in the glovebox with argon atmosphere. Dry toluene (0.2 mL) was delivered via syringe. The resulting mixture was heated at 120 °C for 5 min. A separate 4-mL vial was loaded with **TI** (150 mg, 0.612 mmol), 1,3,5-tribromobenzene (53.7 mg, 0.171 mmol), and K_3PO_4 (217 mg, 1.02 mmol). The reaction vessel was sealed with a screw septum, and evacuated and backfilled with nitrogen three times. Dry toluene (0.7 mL) and the pre-mixed catalyst solution was delivered via syringe. The reaction mixture was heated at 120 °C for 24 h under argon atmosphere. The reaction mixture was cooled to r.t., diluted with CH_2Cl_2 (100 mL), and washed with brine (50 mL). The organic fraction was dried over Na_2SO_4, filtered, and evaporated under reduced pressure. The resulting crude mixture was purified by flash column chromatography on SiO_2 (eluent: CH_2Cl_2/hexane (1:1, v/v) → CH_2Cl_2 only) to afford **3** as a white solid (130 mg, 0.161 mmol, yield

= 95%). ^{1}H NMR (850 MHz, CDCl$_3$, 298 K): δ 8.30 (s, 3H), 7.43 (m, 12H), 7.05 (m, 12H), 5.55 (s, 6H). ^{13}C NMR (214 MHz, CDCl$_3$, 298 K): δ 157.21, 144.36, 141.65, 126.00, 124.50, 104.64, 46.67. FT-IR (ATR, cm^{-1}): 3065, 2324, 2163, 2052, 1982, 1912, 1611, 1563, 1505, 1476, 1457, 1410, 1309, 1254, 1193, 1155, 1143, 1078, 1023, 977, 931, 912, 885, 854, 823, 779, 739, 729, 705, 675, 634, 616. HRMS (ESI, m/z) calcd. for C$_{54}$H$_{33}$N$_9$Na [M + Na]$^+$ 830.2751 , found 830.2755. m.p. > 400 °C.

4) PXRD Experiments

General Considerations for PXRD Measurements. Synchrotron powder X-ray diffraction data were obtained in transmission mode as Debye–Scherrer pattern with 100 mm sample-to-detector distance and 60 s exposure time on a Rayonix MX225HS CCD area detector with a fixed wavelength ($\lambda = 1.20000$ Å) on BL2D-SMC at Pohang Accelerator Laboratory (PAL) in Korea. The PAL BL2D-SMDC program[6] was used for data collection. The Fit2D program[7] was used for the conversion of integrated two-dimensional (2-D) patterns to one-dimensional (1-D) patterns, wavelength and detector refinement, and the calibration measurement of a National Institute of Standards and Technology (NIST) Si 640c standard sample. The initial powder X-ray diffraction data (Fig. S1d) was recorded on a LYNXEYE XE detector using CuKα radiation ($\lambda = 1.5406$ Å) on D8 ADVANCE with DAVINCI. The 2θ values in the plot were adjusted to 1.2000 Åusing the Bragg's law.

Preparation of Bulk Powder Samples of 1A, 1B, 1C, and 1Z. A portion of pentane (40 mL) was poured rapidly into a chloroform solution of **1** (1.0 mg/mL, 10 mL), and the mixture was vigorously agitated to induce immediate precipitation. The PXRD patterns of the isolated solid material confirmed that the bulk is comprised of the **1A** phase. Drying under reduced pressure (0.1 mbar) at $T = 373$ K converted **1A** to **1C**. On the other hand, one-day aging of **1A** in the mother liquor transformed it into **1B**, as analyzed by PXRD on the harvested sample. Drying of **1B** powder sample under reduced pressure (0.1 mbar) at $T = 373$ K yielded activated **1B** with a small amount of **1C**. Drying of **1B** powder at $T = 483$ K in a 0.4-mm diameter (wall thickness = 0.01 mm) capillary (Hampton Research Inc. glass number 50) transformed it into **1Z**.

In Situ Variable Pressure PXRD Measurements. Powder samples were packed in a 0.4-mm diameter (wall thickness = 0.01 mm) capillary (Hampton Research Inc. glass number 50) in the presence of solvent. In situ variable pressure PXRD measurements were carried out by using a custom-built apparatus equipped with vacuum manifold and goniometer head. Before data collection, sample powder was outgassed at $T = 393$ K under vacuum until its PXRD pattern consistently showed a pure phase. After activation, the sample was cooled to the measurement temperature by using a cryostream at $T = 90$ K under vacuum. At each step of variable pressure PXRD measurement, nitrogen gas (ca. 99.9999%) was introduced to the capillary. A fine adjustable needle valve (Swagelok Company) was used to control the pressure from vacuum to 756 torr. At the designated pressure, the sample was allowed to equilibrate for at least 10–15 min prior to recording the diffraction patterns.

Variable Temperature PXRD Measurements. Crystalline samples were gently ground in an agate mortar and packed in a 0.4-mm diameter (wall thickness = 0.01 mm) capillary (Hampton Research Inc. glass number 50) in the presence of solvent. For the variable temperature PXRD measurements, the capillary tube was attached to a custom-made goniometer head with an opening to air and temperature-controlled N_2 stream with a blower equipment (Leister LE MINI Sensor Kit with 5-mm nozzle). The diffraction patterns were measured by varying the temperature from $T = 25$ to 325 °C. At the targeted temperature, the sample was allowed to equilibrate for at least 10–15 min prior to recording the diffraction patterns.

---

[6] J. W. Shin, K. Eom and D. Moon, BL2D-SMC, the supramolecular crystallography beamline at the Pohang Light Source II, Korea. *J. Synchrotron Rad.*, 2016, **23**, 369–373.

[7] Fit2D program: Andy Hammersley (E-mail: hammersley@esrf.fr), ESRF; 6 RUE JULES HOROWITZBP 22038043 GRENOBLE CEDEX 9FRANCE.

5) SC-XRD Experiments

Single-Crystal X-ray Crystallographic Studies on 1A. Single crystals of **1A** and **1B** were prepared by vapor diffusion of pentane into a chloroform solution of **1**. A colorless needle-shaped crystal of **1A** (approximate dimensions $0.12 \times 0.08 \times 0.04$ mm^3) was isolated by a nylon loop with Parabar 10312 (Hampton Research Inc.), and mounted on a PHOTON 100 CMOS diffractometer. The data collection was carried out using CuKα radiation and the crystal was kept at $T = 223(2)$ K. A total 36539 reflections were measured ($15.430° \leq 2\theta \leq 154.724°$). The structure was solved with SHELXT[8] using the intrinsic phasing method, and refined by full-matrix least-squares calculation with SHELXL[9] package of OLEX2.[10] All non-hydrogen atoms were refined anisotropically. A total of 3900 unique reflections were used in all calculations. The final $R1$ was 0.1200 ($I \geq 2\sigma(I)$) and $wR2$ was 0.3248 (all data). $C_{38}H_{24}N_6 \cdot 2(C_5H_{12})$, $M = 708.92$ g/mol, monoclinic, $P2_1/c$ (no. 14), $a = 11.9199(8)$ Å, $b = 6.4841(4)$ Å, $c = 24.7395(15)$ Å, $\alpha = 90°$, $\beta = 91.495(4)°$, $\gamma = 90°$, $V = 1911.5(2)$ Å^3, $Z = 2$, $D_c = 1.232$ g/cm^3. CCDC: 1980363.

Single-Crystal X-ray Crystallographic Studies on 1A with Disordered Lattice Solvent Molecules Squeezed. The final refinements of **1A** were performed using the SQUEEZE routine of PLATON package[11] with the modification of the structure factors for the contribution of the disordered lattice solvent electron densities. A total 3968 unique reflections were used in all calculations. The final $R1$ was 0.0890 ($I \geq 2\sigma(I)$) and $wR2$ was 0.2520 (all data). $C_{38}H_{24}N_6$, $M = 564.63$ g/mol, monoclinic, $P2_1/c$ (no. 14), $a = 11.9199(8)$ Å, $b = 6.4841(4)$ Å, $c = 24.7395(15)$ Å, $\alpha = 90°$, $\beta = 91.495(4)°$, $\gamma = 90°$, $V = 1911.5(2)$ Å^3, $Z = 2$, $D_c = 0.981$ g/cm^3. CCDC: 1980364.

Single-Crystal X-ray Crystallographic Studies on 1B. A colorless needle-shaped crystal of **1B** (approximate dimensions $0.3 \times 0.07 \times 0.05$ mm^3) was coated with Parabar 10312 (Hampton Research Inc.) to mount on the micro-loop under cold nitrogen stream at $T = 100(2)$ K. The diffraction data measured using synchrotron radiation ($\lambda = 0.70000$ Å) employing a PLSII-2D SMC on a Rayonix MX225HS CCD area detector with high precision one-axis goniostat at Pohang Accelerator Laboratory, Korea. The PAL BL2D-SMDC program[6] was used for data collection, and HKL3000sm (Ver.717)[12] was used for cell refinement, reduction, and absorption correction. The structure was solved with SHELXT[8] using intrinsic phasing method, and refined by full-matrix least-squares calculation with SHELXL[9] package of OLEX2.[10] All non-hydrogen atoms were refined anisotropically. A total of 11925 reflections were measured ($2.572° \leq 2\theta \leq 49.998°$). A total of 6007 unique reflections were used in all calculations. The final $R1$ was 0.1136 ($I \geq 2\sigma(I)$) and $wR2$ was 0.3197 (all data). $C_{38}H_{24}N_6 \cdot C_5H_{12}$, $M = 636.78$ g/mol, triclinic, $P\bar{1}$ (no. 2), $a = 6.3260(13)$ Å, $b = 15.778(3)$ Å, $c = 16.684(3)$ Å, $\alpha = 81.36(3)°$, $\beta = 89.31(3)°$, $\gamma = 88.89(3)°$, $V = 1646.0(6)$ Å^3, $Z = 2$, $D_c = 1.285$ g/cm^3. CCDC: 1980365.

Single-Crystal X-ray Crystallographic Studies on 1B with Disordered Lattice Solvent Molecules Squeezed. The final refinements of **1B** were performed using the SQUEEZE routine of PLATON package[11] with the modification of the structure factors for the contribution of the disordered lattice solvent electron densities. A total of 6007 unique reflections were used in all

[8]G. M. Sheldrick, SHELXT – Integrated space-group and crystal-structure determination. *Acta Cryst.*, 2015, **A71**, 3–8.

[9]G. M. Sheldrick, Crystal structure refinement with SHELXL. *Acta Cryst.* 2015, **C71**, 3–8.

[10]O. V. Dolomanov, L. J. Bourhis, R. J. Gildea, J. A. K. Howard and H. Puschmann, OLEX2: a complete structure solution, refinment and analysis program. *J. Appl. Cryst.*, 2009, **42**, 339–341.

[11]A. L. Spek, Structural validation in chemical crystallography. *Acta Cryst.*, 2009, **D65**, 148–155.

[12]Z. Otwinowski and W. Minor, Processing of X-ray diffraction data collected in oscillation mode. *Methods Enzymol.*, 1997, **276**, 307–326.

calculations. The final $R1$ was 0.1022 ($I \geq 2\sigma(I)$) and $wR2$ was 0.045 (all data). $C_{38}H_{24}N_6$, M = 564.63 g/mol, triclinic, $P\bar{1}$ (no. 2), a = 6.3260(13) Å, b = 15.778(3) Å, c = 16.684(3) Å, α = 81.36(3)°, β = 89.31(3)°, γ = 88.89(3)°, V = 1646.0(6) Å^3, Z = 2, D_c = 1.139 g/cm^3. CCDC: 1980366.

Single-Crystal X-ray Crystallographic Studies on 1C. Single crystals of **1C** were prepared by vacuum drying (T = 373 K) of the crystalline material that was precipitated by vapor diffusion of pentane into a chloroform solution of **1**. A colorless needle-shaped crystal of **1C** (approximate dimensions 0.1 × 0.02 × 0.02 mm^3) was coated with Parabar 10312 (Hampton Research Inc.) to mount on the micro-loop under cold nitrogen stream at T = 223(2) K. The diffraction data measured using synchrotron radiation (λ = 0.65303 Å) employing a PLSII-2D SMC on a Rayonix MX225HS CCD area detector with high precision one-axis goniostat at Pohang Accelerator Laboratory, Korea. The PAL BL2D-SMDC program[6] was used data collection, and HKL3000sm (Ver.717)[12] was used for cell refinement, reduction, and absorption correction. The structure was solved with SHELXT[8] using intrinsic phasing method, and refined by full-matrix least-squares calculation with SHELXL[9] package of OLEX2.[10] All non-hydrogen atoms were refined anisotropically. A total of 13497 reflections were measured (3.108° ≤ 2θ ≤ 53.994°). A total of 4067 unique reflections were used in all calculations. The final $R1$ was 0.0753 ($I \geq 2\sigma(I)$) and $wR2$ was 0.2131 (all data). $C_{38}H_{24}N_6$, M = 564.63 g/mol, monoclinic, $P2_1/n$ (no. 14), a = 9.2440(19) Å, b = 6.6490(13) Å, c = 24.353(5) Å, α = 90°, β = 98.58(3)°, γ = 90°, V = 1480.1(5) Å^3, Z = 2, D_c = 1.267 g/cm^3. CCDC: 1980367.

Single-Crystal X-ray Crystallographic Studies on 1Z. Single crystals of **1Z** were prepared by heating **1B** powder sample confined in a capillary at T > 448 K. A colorless needle-shaped crystal of **1Z** (approximate dimensions 0.013 × 0.008 × 0.002 mm^3) was coated with Parabar 10312 (Hampton Research Inc.) to mount on the micro-loop under cold nitrogen stream at T = 298(2) K. The diffraction data was measured using synchrotron radiation (λ = 0.70000 Å) employing a PLSII-2D SMC on a Rayonix MX225HS CCD area detector with high precision one-axis goniostat at Pohang Accelerator Laboratory, Korea. The PAL BL2D-SMDC program[6] was used data collection, and HKL3000sm (Ver.717)[12] was used for cell refinement, reduction, and absorption correction. The structure was solved with SHELXT[8] using intrinsic phasing method, and refined by full-matrix least-squares calculation with SHELXL[9] package of OLEX2.[10] All non-hydrogen atoms were refined anisotropically. A total of 15059 reflections were measured (3.772° ≤ 2θ ≤ 49.670°). A total of 4677 unique reflections were used in all calculations. The final $R1$ was 0.0659 ($I \geq 2\sigma(I)$) and $wR2$ was 0.1850 (all data). $C_{38}H_{24}N_6$, M = 564.63 g/mol, monoclinic, $P2_1/n$ (no. 14), a = 6.4290(13) Å, b = 14.653(3) Å, c = 15.517(3) Å, α = 90°, β = 94.96(3)°, γ = 90°, V = 1456.3(5) Å^3, Z = 2, D_c = 1.288 g/cm^3. CCDC: 1980368.

Single-Crystal X-ray Crystallographic Studies on 2. Single crystals of **2** were prepared by vapor diffusion of pentane into a chloroform solution of **2**. A colorless block-shaped crystal of **2** (approximate dimensions 0.25 × 0.165 × 0.081 mm^3) was isolated by a nylon loop with Parabar 10312 (Hampton Research Inc.), and mounted on a four-circle diffractometer. The data collection was carried out using CuKα radiation and the crystal was kept at T = 93(2) K. A total 22039 reflections were measured (8.844° ≤ 2θ ≤ 157.79°). The structure was solved with SHELXT[8] using the intrinsic phasing method, and refined by full-matrix least-squares calculation with SHELXL[9] package of OLEX2.[10] All non-hydrogen atoms were refined anisotropically. A total of 7391 unique reflections were used in all calculations. The final $R1$ was 0.0523 ($I \geq 2\sigma(I)$) and $wR2$ was 0.1410 (all data). $C_{38}H_{24}N_6 \cdot 2(CHCl_3)$, M = 803.37 g/mol, triclinic, $P\bar{1}$ (no. 2), a = 11.6072(2) Å, b = 11.69065(19) Å, c = 15.3099(2) Å, α = 100.1144(13)°, β = 104.4568(15)°, γ = 112.6428(16)°, V = 1768.75(6) Å^3, Z = 2, D_c = 1.508 g/cm^3. CCDC: 2048700.

Single-Crystal X-ray Crystallographic Studies on 3. Single crystals of **3** were prepared by vapor diffusion of pentane into a chloroform solution of **3**. A colorless needle-shaped crystal of **3** (approximate dimensions $0.57 \times 0.089 \times 0.057$ mm^3) was isolated by a nylon loop with Parabar 10312 (Hampton Research Inc.), and mounted on a four-circle diffractometer. The data collection was carried out using CuKα radiation and the crystal was kept at $T = 93(2)$ K. A total 1365 reflections were measured ($7.314° \leq 2\theta \leq 157.302°$). The structure was solved with SHELXT[8] using the intrinsic phasing method, and refined by full-matrix least-squares calculation with SHELXL[9] package of OLEX2.[10] All non-hydrogen atoms were refined anisotropically. A total of 10333 unique reflections were used in all calculations. The final $R1$ was 0.0797 ($I \geq 2\sigma(I)$) and $wR2$ was 0.2517 (all data). $C_{54}H_{33}N_9 \cdot 1.6(CHCl_3)$, $M = 988.88$ g/mol, triclinic, $P\bar{1}$ (no. 2), $a = 11.7152(3)$ Å, $b = 12.5774(3)$ Å, $c = 17.5509(6)$ Å, $\alpha = 99.811(2)°$, $\beta = 93.572(2)°$, $\gamma = 101.070(2)°$, $V = 2488.73(12)$ Å^3, $Z = 2$, $D_c = 1.333$ g/cm^3. CCDC: 2048701.

6) Validation Reply Forms

Validation Reply Form: Detailing any alerts in the **1A** crystal structure.
_vrf_PLAT097_ALERT_2_B
Problem: Large Reported Max. (Positive) Residual Density 0.82 eA-3
Response: The large channels within **1A** were occupied by heavily disordered solvent molecules that could not be modeled perfectly. This deviation of the model from the observed electron density resulted in such residual densities. While this problem could be solved by squeezing all the disordered solvent molecules, simulation of powder diffraction patterns required unprocessed raw data. We thus decided to report both "unsqueezed" and "squeezed" crystallographic data.

Validation Reply Form: Detailing any alerts in the **1Z** crystal structure.
_vrf_PLAT026_ALERT_3_B
Problem: Ratio Observed / Unique Reflections (too) Low ... 33% Check
Response: The diffraction spots' weak intensities were inevitable due to the extremely small crystal size of **1Z** ($0.013 \times 0.008 \times 0.002$ mm^3).

7) Supplementary Tables

Table S1. Hydrogen bonds for **1A** [Å and °]

D–H⋯A	d(D–H)	d(H⋯A)	d(D⋯A)	∠DHA
C(17)–H(17)⋯N(1)	0.94	2.51	2.830(7)	100.0
C(19)–H(19)⋯N(3)	0.94	2.53	2.839(6)	99.1
C(13)–H(13)⋯N(3)#2	0.99	2.38	3.366(5)	173.5

Symmetry transformations used to generate equivalent atoms:
#1 -x+1,-y,-z+1   #2 x,y+1,z

Table S2. Hydrogen bonds for **1A_squeezed** [Å and °]

D–H⋯A	d(D–H)	d(H⋯A)	d(D⋯A)	∠DHA
C(13)–H(13)⋯N(3)#2	0.99	2.38	3.366(4)	173.5
C(1)–H(1)⋯N(1)	0.94	2.51	2.831(5)	100.0
C(3)–H(3)⋯N(3)	0.94	2.51	2.829(5)	99.7

Symmetry transformations used to generate equivalent atoms:
#1 -x+2,-y,-z+1   #2 x,y+1,z

Table S3. Hydrogen bonds for **1B** [Å and °]

D–H⋯A	d(D–H)	d(H⋯A)	d(D⋯A)	∠DHA
C(6A)–H(6A)⋯N(1A)#3	1.00	2.37	3.363(5)	174.3
C(13B)–H(13B)⋯N(3B)#4	1.00	2.37	3.371(5)	174.4

Symmetry transformations used to generate equivalent atoms:
#1 -x,-y,-z+1   #2 -x+1,-y+1,-z+1   #3 x+1,y,z   #4 x-1,y,z

Table S4. Hydrogen bonds for **1B_squeezed** [Å and °]

D–H⋯A	d(D–H)	d(H⋯A)	d(D⋯A)	∠DHA
C(6A)–H(6A)⋯N(1A)#3	1.00	2.37	3.367(4)	174.3
C(13B)–H(13B)⋯N(3B)#4	1.00	2.37	3.369(4)	174.5

Symmetry transformations used to generate equivalent atoms:
#1 -x,-y,-z+1   #2 -x+1,-y+1,-z+1   #3 x+1,y,z   #4 x-1,y,z

Table S5. Hydrogen bonds for **1C** [Å and °]

D–H$\cdots$A	d(D–H)	d(H$\cdots$A)	d(D$\cdots$A)	∠DHA
C(13)–H(13)$\cdots$N(3)#2	0.99	2.47	3.391(3)	154.4
C(3)–H(3)$\cdots$N(3)	0.94	2.51	2.825(3)	99.8

Symmetry transformations used to generate equivalent atoms:
#1 -x+2,-y,-z+1   #2 x,y+1,z

Table S6. Hydrogen bonds for **1Z** [Å and °]

D–H$\cdots$A	d(D–H)	d(H$\cdots$A)	d(D$\cdots$A)	∠DHA
C(13)–H(13)$\cdots$N(1)#2	0.98	2.45	3.415(3)	170.0

Symmetry transformations used to generate equivalent atoms:
#1 -x,-y+1,-z+1   #2 x+1,y,z

Table S7. Crystallographically determined metric parameters for C–H$\cdots\pi$ interaction observed in four polymorphs of **1**. The central phenyl, triazole, and pheripheral phenyl rings are labeled as plane A, B, and C. Key C–H$\cdots\pi$ interactions are highlighted with gray boxes.

	(C–H)$_C\cdots\pi_A$ (Å)		θ_{AC} (deg)
	Carbon to rms plane	Carbon to plane centroid	
1A	3.594(8)	4.463(5)	63.1(2)
1B	2.982(8)	4.781(4)	74.08(14)
1C	3.517(4)	3.681(3)	63.21(11)
1Z	3.305(4)*	3.785(3)	27.10(10)

	(C–H)$_C\cdots\pi_B$ (Å)		θ_{BC} (deg)
	Carbon to rms plane	Carbon to plane centroid	
1A	3.441(4)	3.505(4)	57.63(13)
1B	3.485(4)	3.527(4)	60.72(13)
1C	3.410(3)	3.447(3)	64.20(10)
1Z	3.404(3)	3.697(3)	45.28(9)

	(C–H)$_C\cdots\pi_C$ (Å)		θ_{CC} (deg)
	Carbon to rms plane	Carbon to plane centroid	
1A	3.592(5)	3.675(4)	45.48(19)
1B	3.502(4)	3.561(4)	43.26(10)
1C	3.629(3)	3.942(3)	84.75(9)
1C	3.430(5)	4.363(3)	84.75(9)
1Z	3.665(4)	3.703(4)	85.16(11)
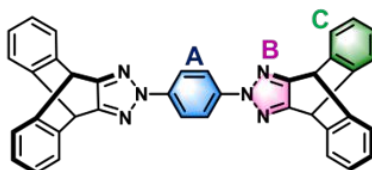
* In this case, the interplanar angle between the two π-surfaces is relatively small (27.10(10)°). As such, the interaction between the two π-planes might be better described as $\pi\cdots\pi$ interaction, rather than C–H$\cdots\pi$ interaction. The interplanar distance, measured between the centroid of one aromatic ring and the mean plan of the other aromatic ring, is 3.774(2) Å.

Table S8. Metric parameters of relevance to the cavity dimensions.

Polymorphs of **1**	Unit cell density (g/cm^3)	Solvent-accessible surface area (m^2/g)^a	Maximum radius of a spherical probe to fit inside the channels (Å)
1A	0.981	1629	2.6
1B	1.139	1010	1.9
1C	1.267	140	1.3
1Z	1.288	45	1.3

^{a} Determined by using a spherical probe of r=1 Å probe.

Table S9. Summary of X-ray crystallographic data of **1A**.

	$1 \cdot 2(C_5H_{12})$
Chemical formula	$C_{38}H_{24}N_6 \cdot 2(C_5H_{12})$
Formula weight	708.92
Crystal system	monoclinic
Space group	$P2_1/c$
Color of crystal	colorless
D_c	1.232 g/cm^3
a (Å)	11.9199(8)
b (Å)	6.4841(4)
c (Å)	24.7395(15)
α (°)	90
β (°)	91.495(4)
γ (°)	90
Volume (Å^3)	1911.5(2)
Z	2
R(int)	0.1136
Final R indices $[I > 2\sigma(I)]$	$R1 = 0.1200, wR2 = 0.2968$
Final R indices [all data]	$R1 = 0.1542, wR2 = 0.3248$
GOF	1.088

Table S10. Summary of X-ray crystallographic data of **1A_squeezed**.

	1
Chemical formula	$C_{38}H_{24}N_6$
Formula weight	564.63
Crystal system	monoclinic
Space group	$P2_1/c$
Color of crystal	colorless
D_c	0.981 g/cm^3
a (Å)	11.9199(8)
b (Å)	6.4841(4)
c (Å)	24.7395(15)
α (°)	90
β (°)	91.495(4)
γ (°)	90
Volume (Å^3)	1911.5(2)
Z	2
R(int)	0.1136
Final R indices $[I > 2\sigma(I)]$	$R1 = 0.0890, wR2 = 0.2342$
Final R indices [all data]	$R1 = 0.1163, wR2 = 0.2520$
GOF	1.070

Table S11. Summary of X-ray crystallographic data of **1B**.

	$1 \cdot C_5H_{12}$
Chemical formula	$C_{38}H_{24}N_6 \cdot C_5H_{12}$
Formula weight	636.78
Crystal system	triclinic
Space group	$P\bar{1}$
Color of crystal	colorless
D_c	1.285 g/cm^3
a (Å)	6.3260(13)
b (Å)	15.778(3)
c (Å)	16.684(3)
α (°)	81.36(3)
β (°)	89.31(3)
γ (°)	88.89(3)
Volume (Å^3)	1646.0(6)
Z	2
R(int)	0.0395
Final R indices $[I > 2\sigma(I)]$	$R1 = 0.1136, wR2 = 0.2996$
Final R indices [all data]	$R1 = 0.1359, wR2 = 0.3197$
GOF	1.218

Table S12. Summary of X-ray crystallographic data of **1B_squeezed**.

	1
Chemical formula	$C_{38}H_{24}N_6$
Formula weight	564.63
Crystal system	triclinic
Space group	$P\bar{1}$
Color of crystal	colorless
D_c	1.139 g/cm^3
a (Å)	6.3260(13)
b (Å)	15.778(3)
c (Å)	16.684(3)
α (°)	81.36(3)
β (°)	89.31(3)
γ (°)	88.89(3)
Volume (Å^3)	1646.0(6)
Z	2
R(int)	0.0395
Final R indices $[I > 2\sigma(I)]$	$R1 = 0.1022, wR2 = 0.2881$
Final R indices [all data]	$R1 = 0.1222, wR2 = 0.3045$
GOF	1.151

Table S13. Summary of X-ray crystallographic data of **1C**.

	1
Chemical formula	$C_{38}H_{24}N_6$
Formula weight	564.63
Crystal system	monoclinic
Space group	$P2_1/n$
Color of crystal	colorless
D_c	1.267 g/cm^3
a (Å)	9.2440(19)
b (Å)	6.6490(13)
c (Å)	24.353(5)
α (°)	90
β (°)	98.58(3)
γ (°)	90
Volume (Å^3)	1480.1(5)
Z	2
R(int)	0.1076
Final R indices [$I > 2\sigma(I)$]	$R1 = 0.0753, wR2 = 0.1795$
Final R indices [all data]	$R1 = 0.1480, wR2 = 0.2131$
GOF	0.931

Table S14. Summary of X-ray crystallographic data of **1Z**.

	1
Chemical formula	$C_{38}H_{24}N_6$
Formula weight	564.63
Crystal system	monoclinic
Space group	$P2_1/n$
Color of crystal	colorless
D_c	1.288 g/cm^3
a (Å)	6.4290(13)
b (Å)	14.653(3)
c (Å)	15.517(3)
α (°)	90
β (°)	94.96(3)
γ (°)	90
Volume (Å^3)	1456.3(5)
Z	2
R(int)	0.2042
Final R indices [$I > 2\sigma(I)$]	$R1 = 0.0659, wR2 = 0.1452$
Final R indices [all data]	$R1 = 0.2053, wR2 = 0.1850$
GOF	0.791

Table S15. Summary of X-ray crystallographic data of **2**.

	2 · 2(CHCl$_3$)
Chemical formula	C$_{40}$H$_{26}$Cl$_6$N$_6$
Formula weight	803.37
Crystal system	triclinic
Space group	$P\bar{1}$
Color of crystal	colorless
D_c	1.508 g/cm^3
a (Å)	11.6072(2)
b (Å)	11.69065(19)
c (Å)	15.3099(2)
α (°)	100.1144(13)
β (°)	104.4568(15)
γ (°)	112.6428(16)
Volume (Å^3)	1768.75(6)
Z	2
R(int)	0.0433
Final R indices [$I > 2\sigma(I)$]	$R1 = 0.0523$, $wR2 = 0.1384$
Final R indices [all data]	$R1 = 0.0550$, $wR2 = 0.1410$
GOF	1.096

Table S16. Summary of X-ray crystallographic data of **3**.

	3 · 1.6(CHCl$_3$)
Chemical formula	C$_{54}$H$_{33}$N$_9$ · 1.6(CHCl$_3$)
Formula weight	998.88
Crystal system	triclinic
Space group	$P\bar{1}$
Color of crystal	colorless
D_c	1.333 g/cm^3
a (Å)	11.7152(3)
b (Å)	12.5774(3)
c (Å)	17.5509(6)
α (°)	99.811(2)
β (°)	93.572(2)
γ (°)	101.070(2)
Volume (Å^3)	2488.73(12)
Z	2
R(int)	0.0606
Final R indices [$I > 2\sigma(I)$]	$R1 = 0.0797$, $wR2 = 0.2420$
Final R indices [all data]	$R1 = 0.0868$, $wR2 = 0.2517$
GOF	1.047

8) Supplementary Figures
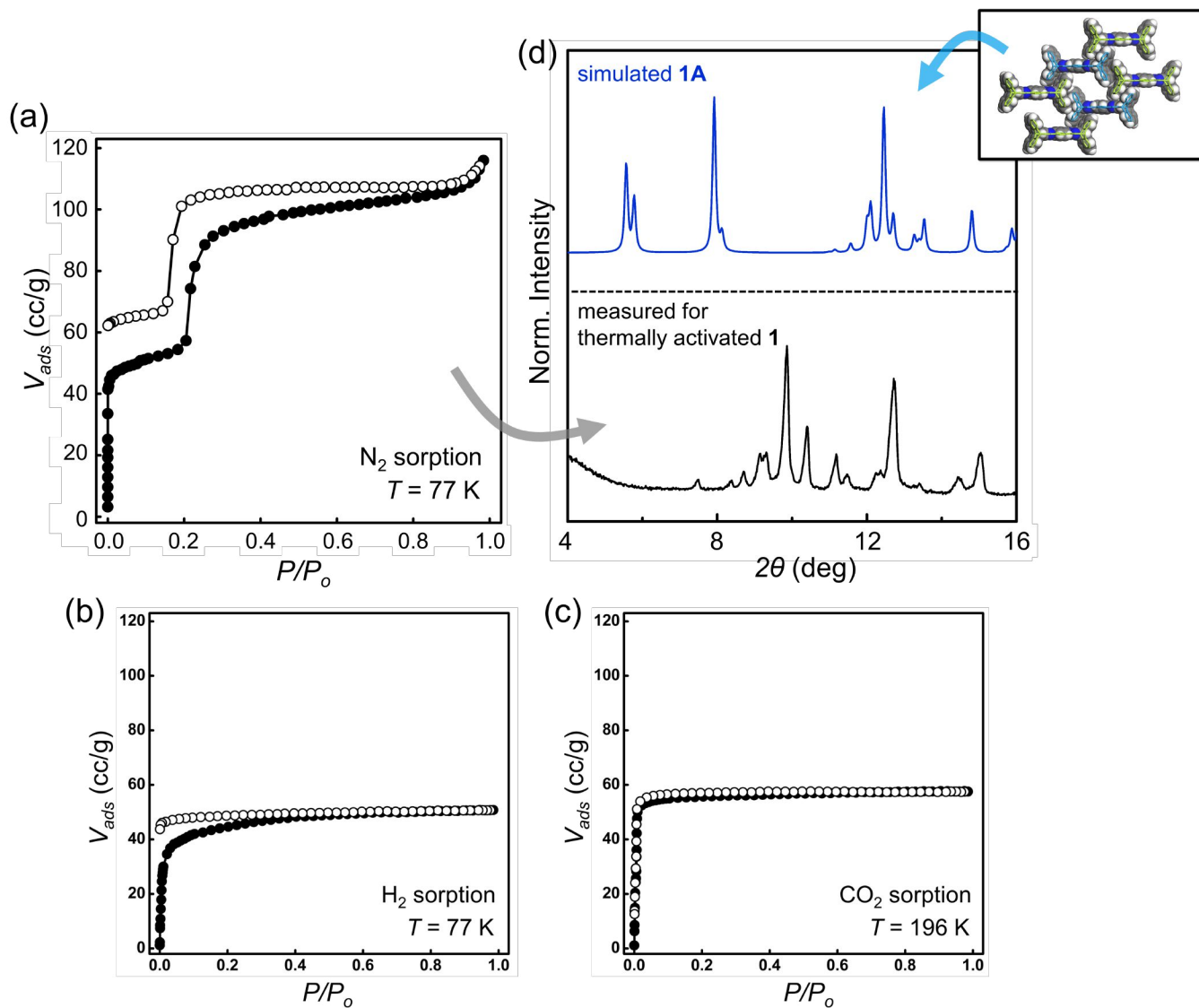
Fig. S1. (a) Initial sorption data of thermally activated crystalline **1** measured for (a) N_2 at $T = 77$ K, (b) H_2 at $T = 77$ K, and (c) CO_2 at $T = 196$ K. (d) Initial PXRD patterns obtained experimentally for thermally activated crystals of **1** (bottom), and simulated with the single-crystal structure of **1A** (top).
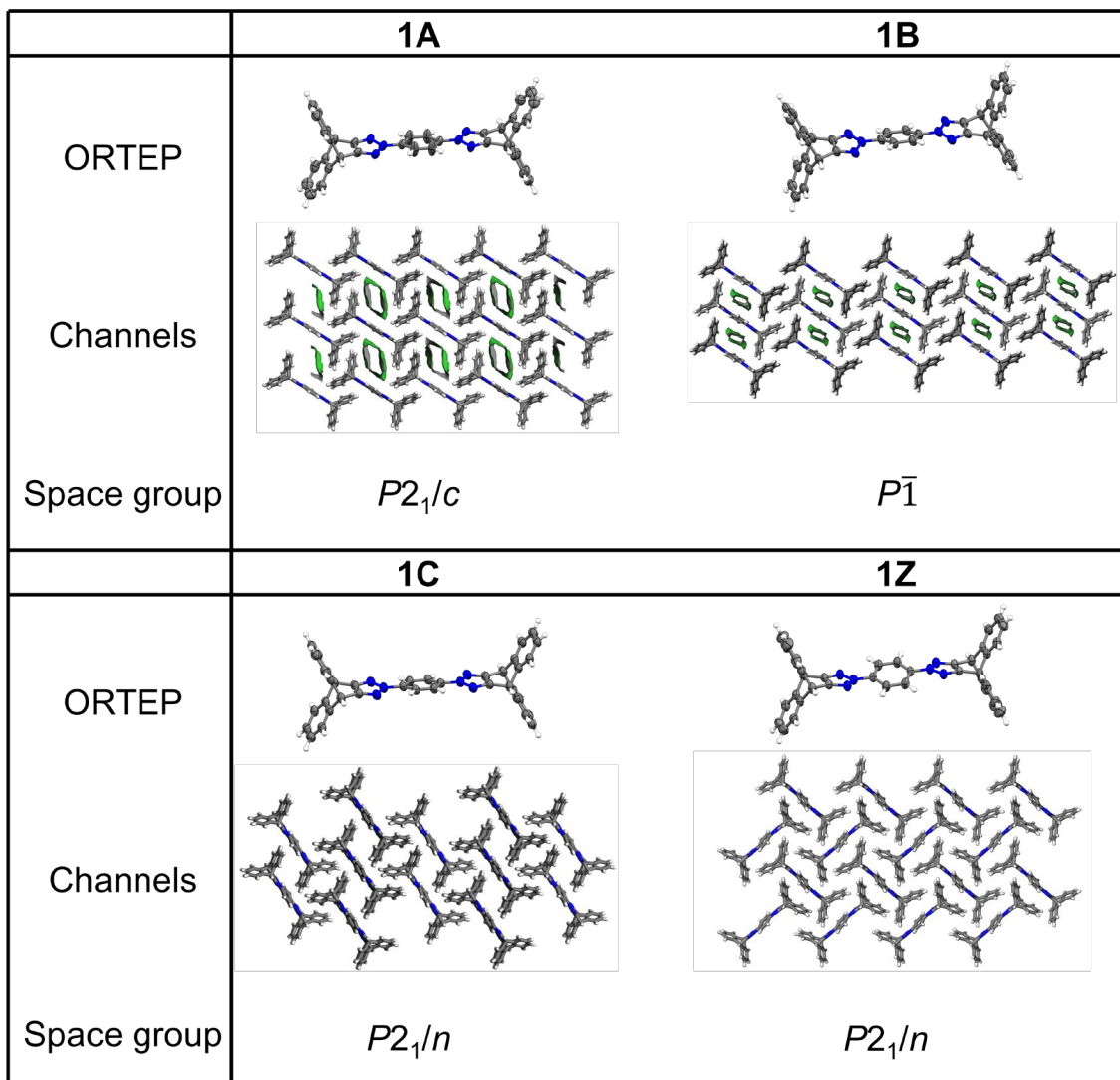
Fig. S2. ORTEP diagrams, packing diagrams, and space groups for different polymorphs of **1**. The ORTEP diagrams were generated with thermal ellipsoids at the 35% probability level. For **1A** and **1B**, packing diagrams were drawn with the solvent-accessible void space visualized by gray and green (inner and outer, respectively) curved planes to show open channels. The surfaces were generated with a $r = 1.4$ Å probe. For **1C** and **1Z**, solvent-accessible surfaces could not be generated, since $r = 1.4$ Å probe cannot access the pores.
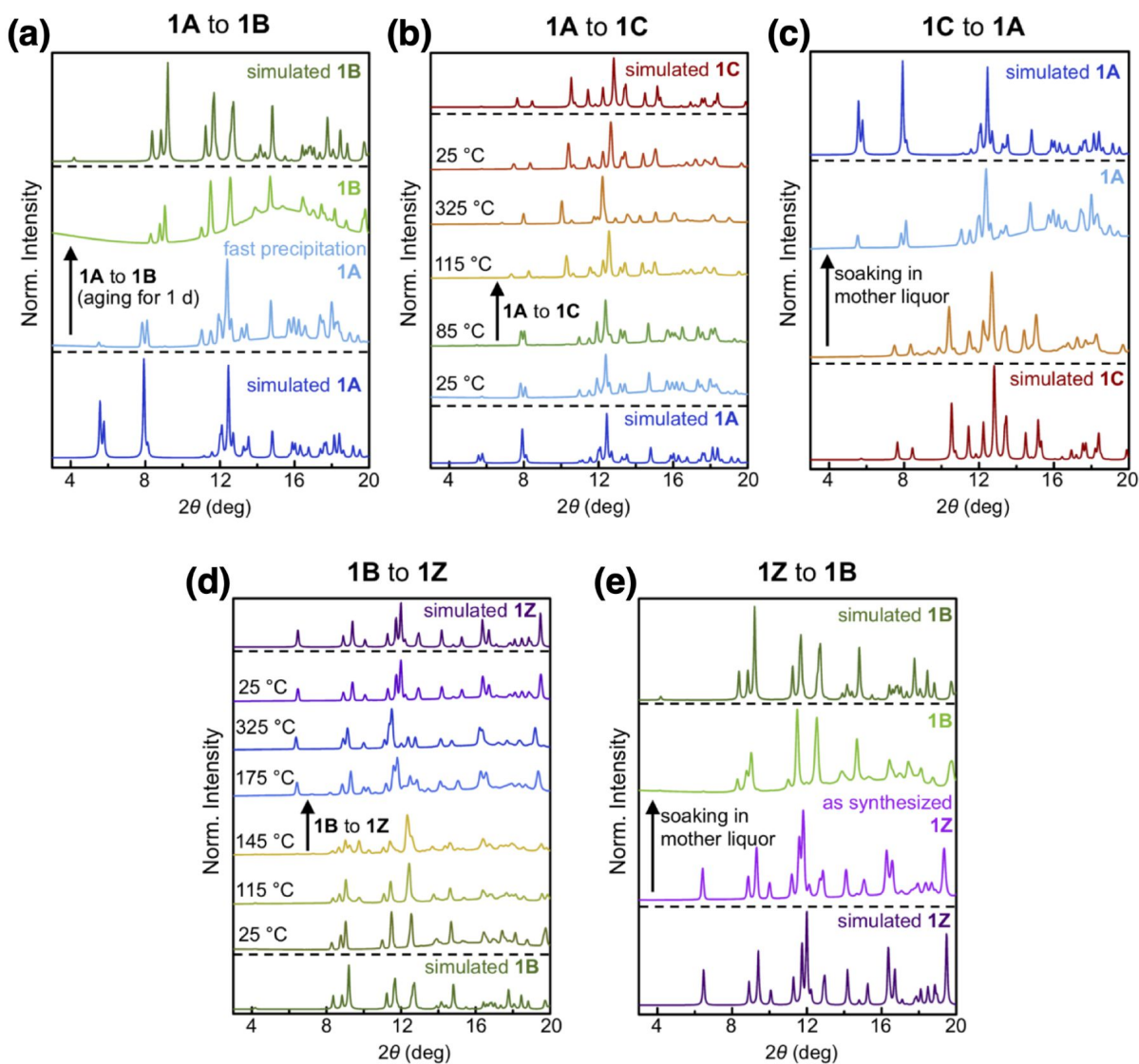
Fig. S3. PXRD pattern changes of **1** recorded during the phase transitions. (a) Changes in the PXRD patterns for **1A** → **1B** transition. (b) Changes in the PXRD patterns for **1A** → **1C** transition. (c) Changes in the PXRD patterns for **1C** → **1A** transition. (d) Changes in the PXRD patterns for **1B** → **1Z** transition. (e) Changes in the PXRD patterns for **1Z** → **1B** transition.
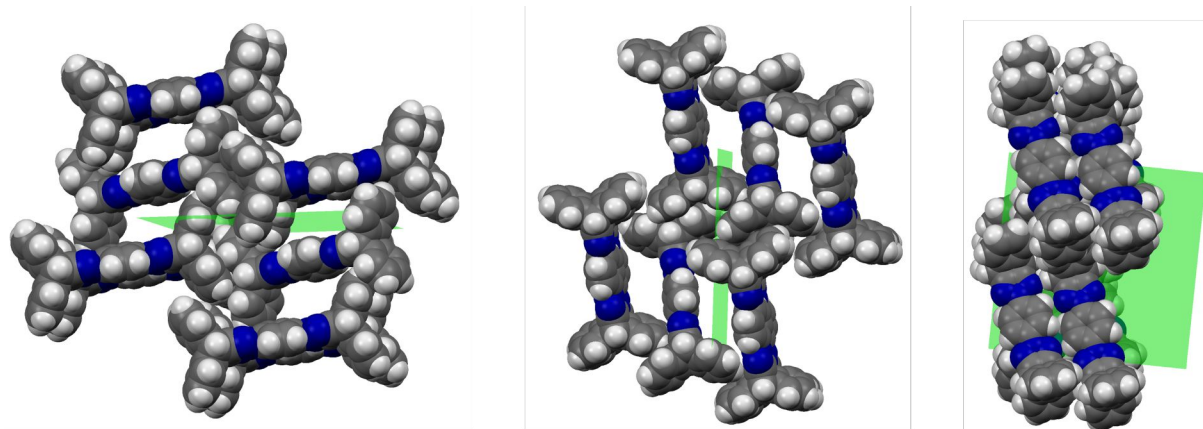
Fig. S4. The (021) plane of **1B** crystal structure viewed from different perspectives.
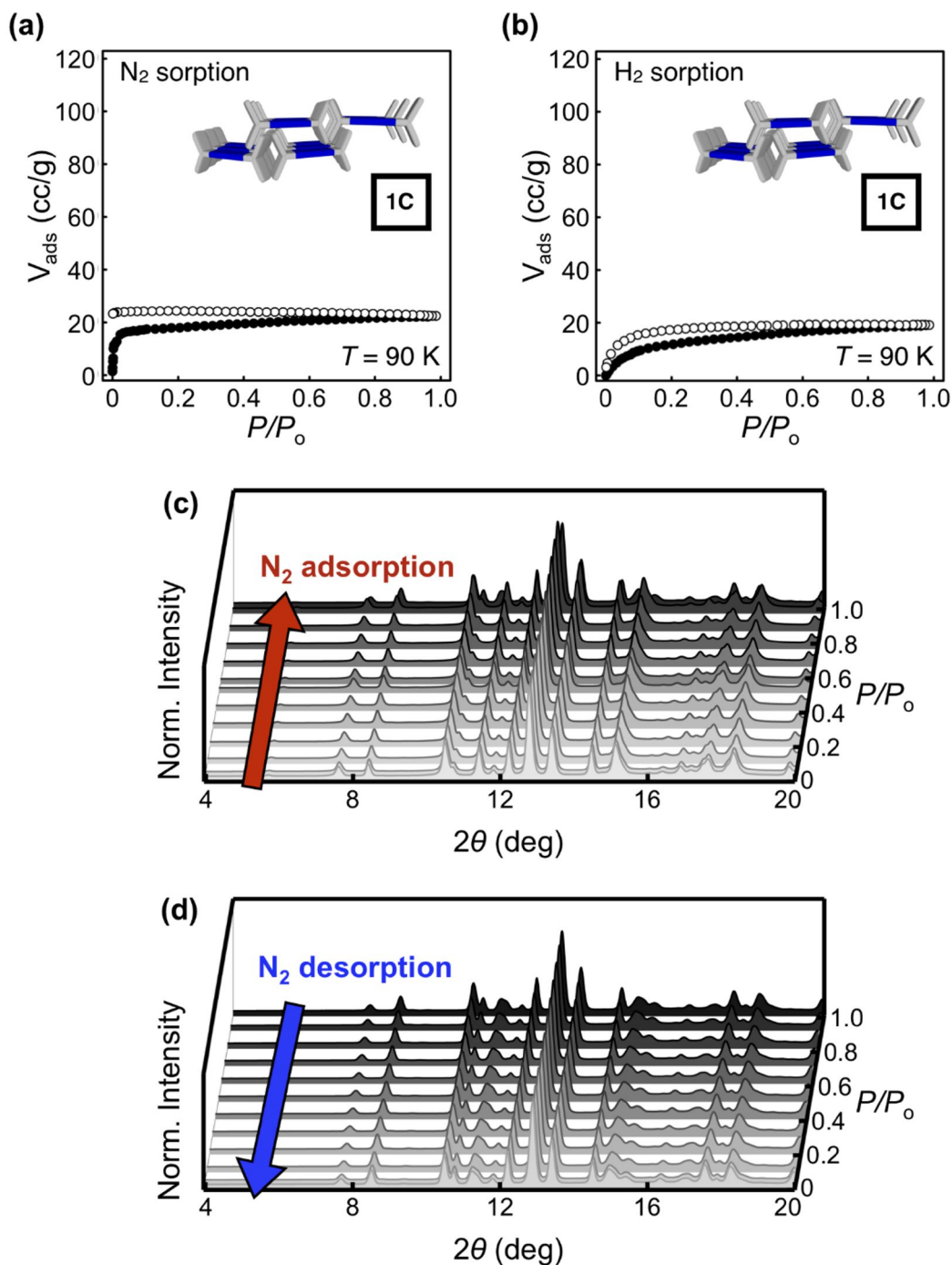
Fig. S5. Adsorption (filled circles) and desorption (empty circles) isotherms of **1C** measured for (a) N_2 and (b) H_2 at $T = 90$ K. (c) PXRD changes of **1C** recorded during the entire N_2 adsorption process. (d) PXRD changes of **1C** recorded during the entire N_2 desorption process. No noticeable changes were observed in the PXRD pattern during the adsorption and desorption cycle.
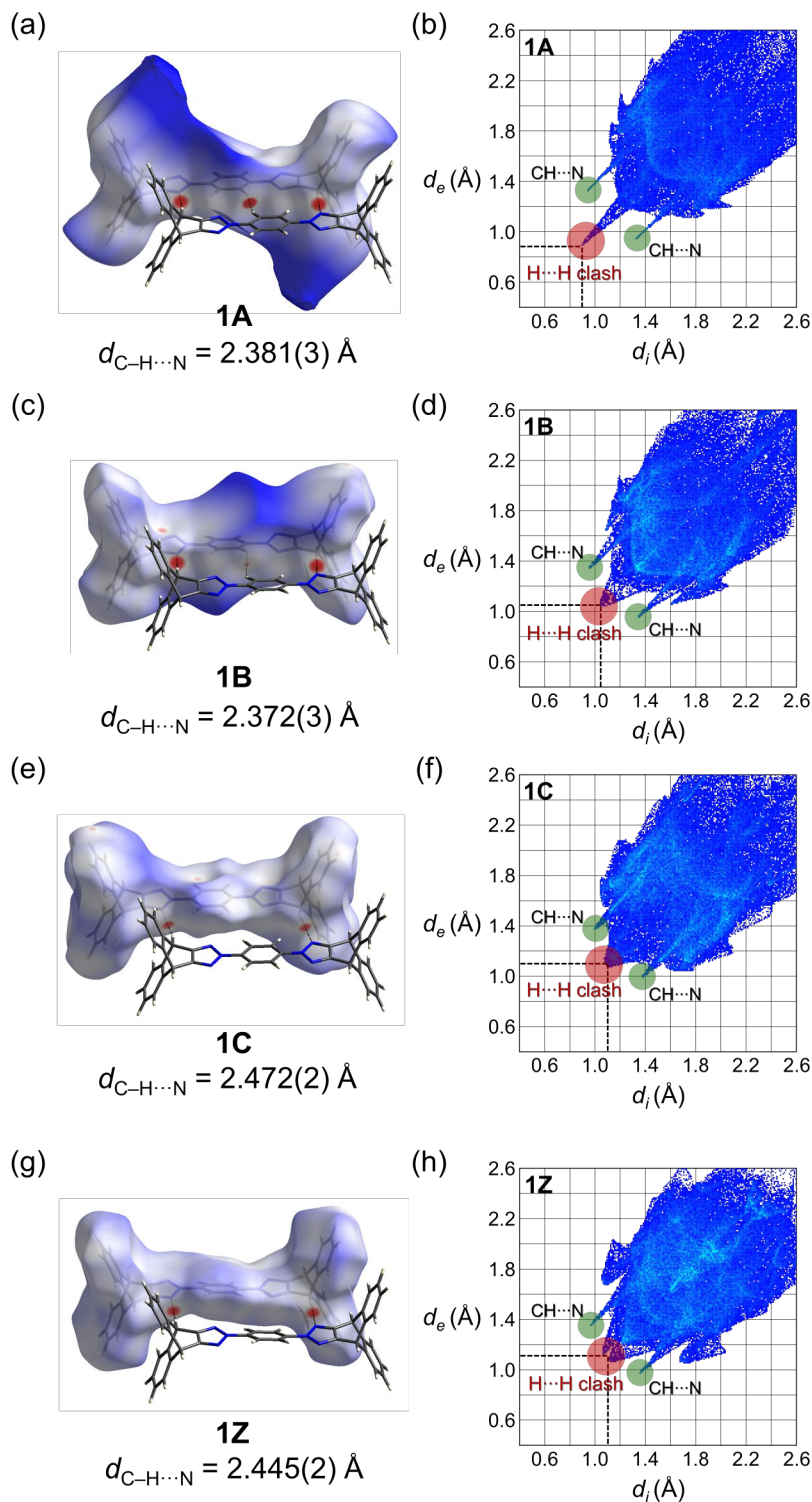
Fig. S6. Hirshfeld surfaces mapped by d_{norm} values for ((a) **1A**, (c) **1B**, (e) **1C**, and (g) **1Z**), and corresponding fingerprint plots ((b) **1A**, (d) **1B**, (f) **1C**, and (h) **1Z**) that highlight lateral assembly of **1**. The C–H$\cdots$N hydrogen bond distances ($d_{\mathrm{C-H}\cdots\mathrm{N}}$) provided under the Hirshfeld surfaces denote the interatomic distance between hydrogen and nitrogen atoms.
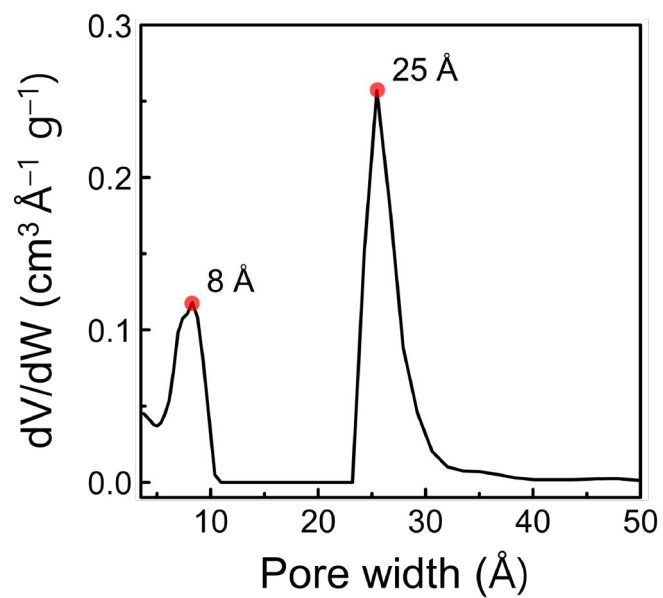
Fig. S7. Pore distribution of activated **1B** calculated from the N_2 sorption isotherm (NLDFT).
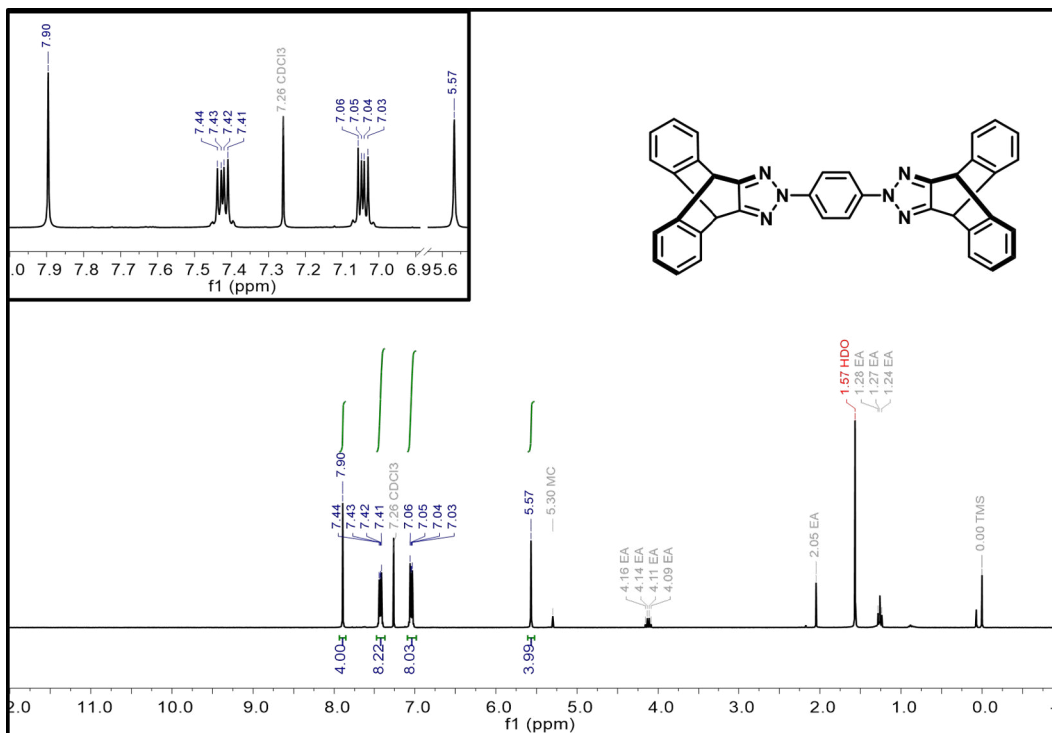
Fig. S8. ^{1}H NMR (300 MHz) spectrum of **1** in CDCl$_3$ ($T = 298$ K).
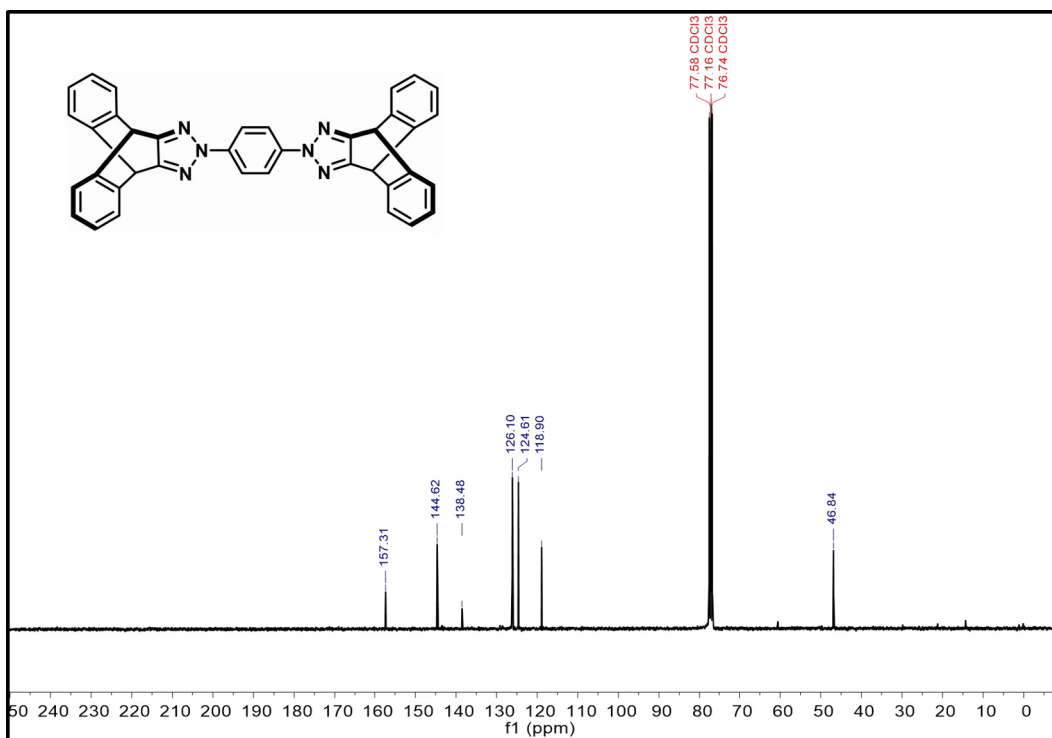
Fig. S9. ^{13}C NMR (75 MHz) spectrum of **1** in CDCl$_3$ ($T = 298$ K).
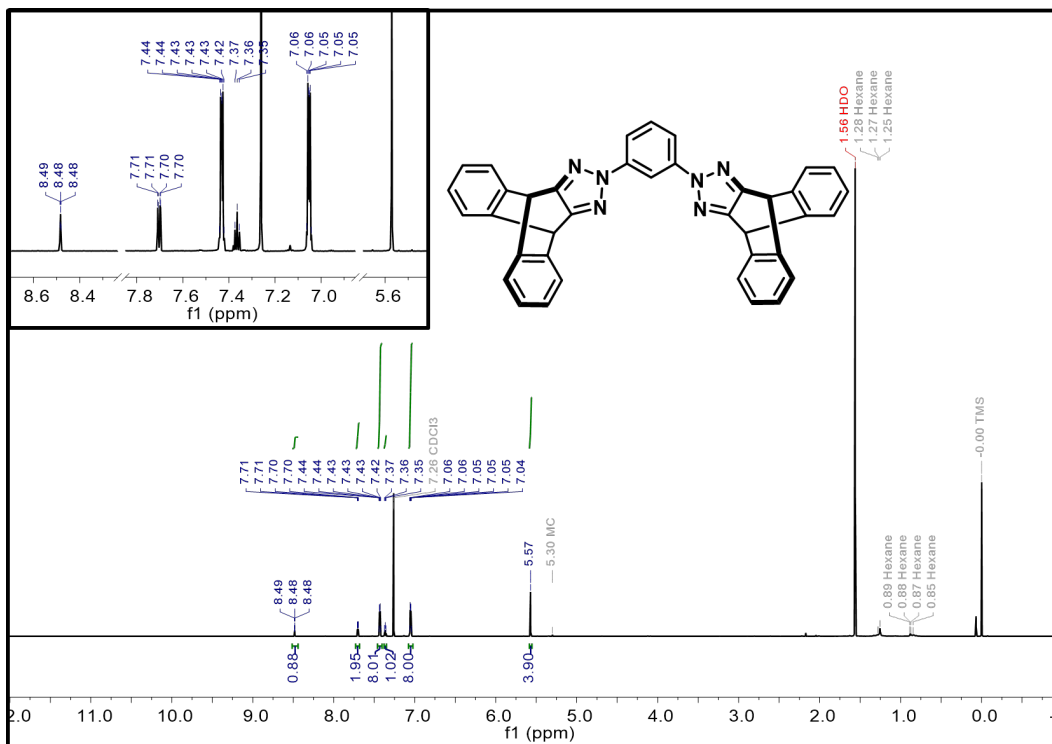
Fig. S10. ^{1}H NMR (850 MHz) spectrum of **2** in CDCl$_3$ ($T = 298$ K).
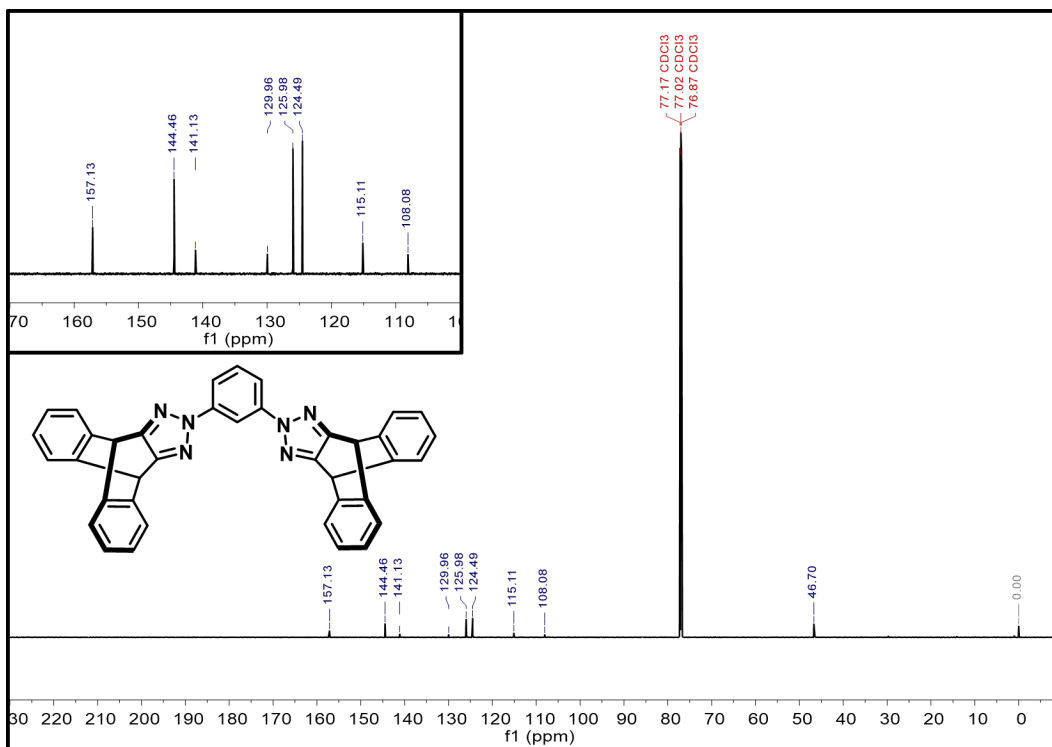
Fig. S11. ^{13}C NMR (214 MHz) spectrum of **2** in CDCl$_3$ ($T = 298$ K).
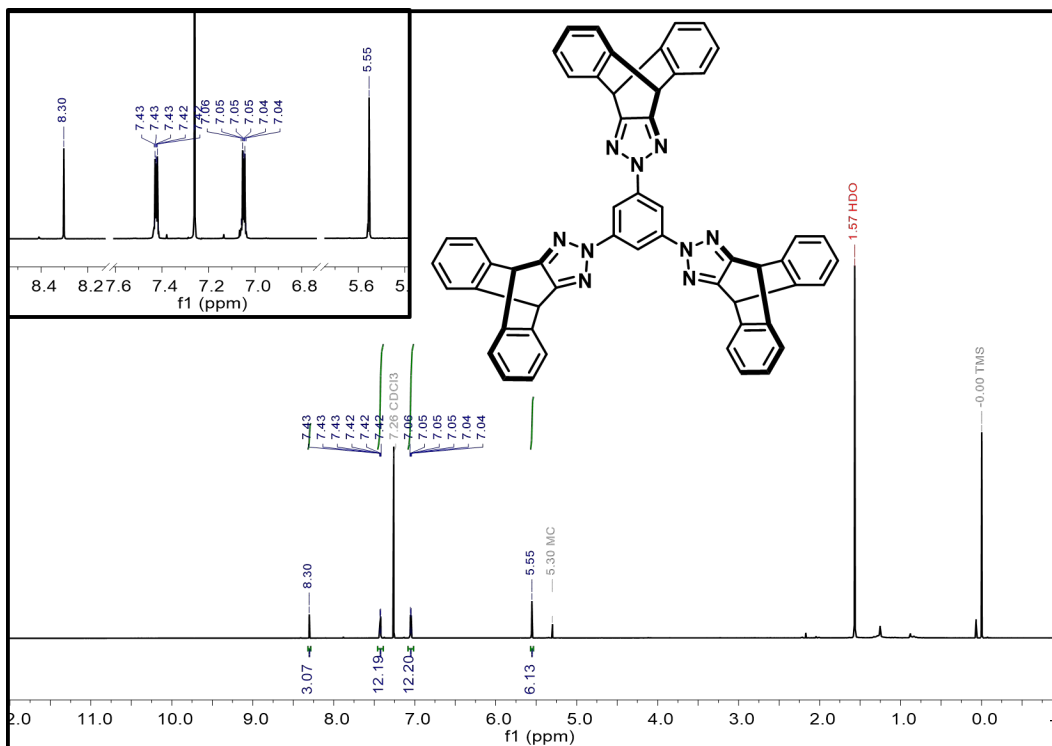
Fig. S12. ^{1}H NMR (850 MHz) spectrum of **3** in CDCl$_3$ (T = 298 K).
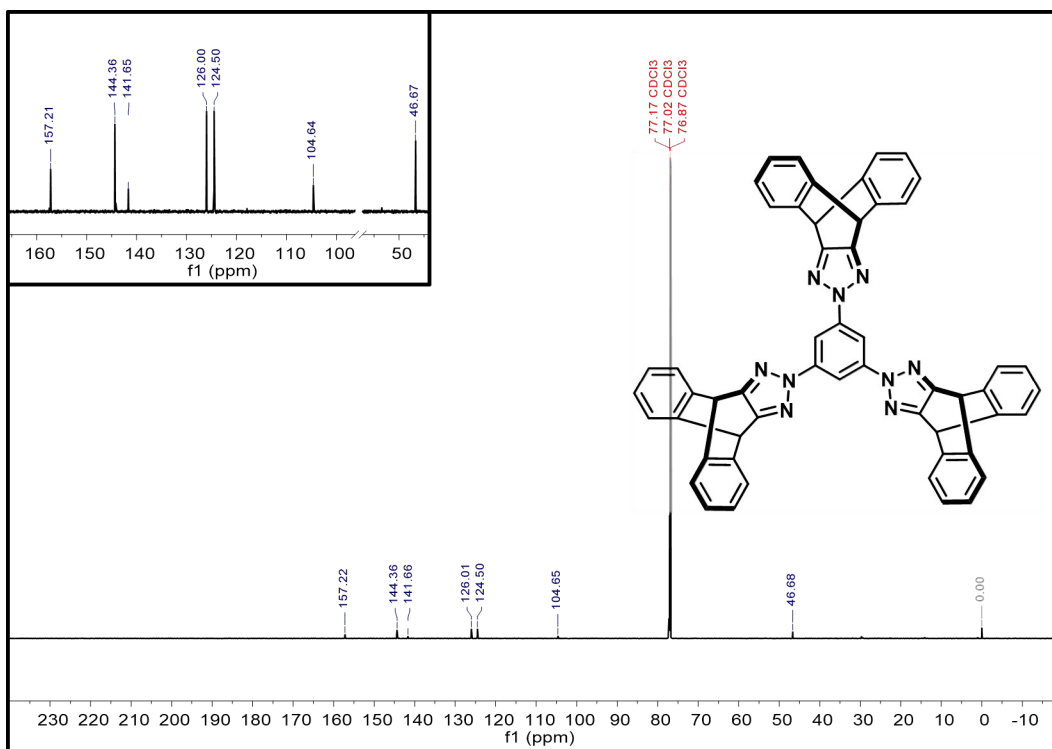
Fig. S13. ^{13}C NMR (214 MHz) spectrum of **3** in CDCl$_3$ (T = 298 K).